NJC

PAPER

View Article Online
View Journal | View Issue

Cite this: *New J. Chem.*, 2018, **42**, 19963

Crystal habit modification of Cu(II) isonicotinate–*N*-oxide complexes using gel phase crystallisation†

Dipankar Ghosh,[a] Katja Ferfolja,[a] Žygimantas Drabavičius,[a] Jonathan W. Steed *[b] and Krishna K. Damodaran *[a]

Received 4th October 2018,
Accepted 1st November 2018

DOI: 10.1039/c8nj05036h

rsc.li/njc

We report the crystallisation of three forms of the copper(II) isonicotinate–*N*-oxide complex and their phase interconversion *via* solvent-mediated crystal-to-crystal transformation. The different forms of the copper complex have been isolated and characterised by single crystal X-ray diffraction. Gel phase crystallisation performed in hydrogels, low molecular weight gels and gels of a tailored gelator showed crystal habit modification. Crystallisation in aqueous ethanol resulted in the concomitant formation of blue (form-I) and green (form-II/IV) crystals while the use of a low molecular weight gel resulted in the selective crystallization of the blue form-I under identical conditions. Comparison of the gel phase and the solution state crystallisation in various solvent compositions reveals that the blue form-I is the thermodynamically stable form under ambient conditions.

Introduction

Supramolecular gels based on low molecular weight gelators (LMWGs)[1–9] have witnessed tremendous growth over the last decade due to their emerging potential applications[5–8] such as dynamic behaviour, use as cell growth media, drug delivery and as media to control crystal growth. Gel phase crystallisation in hydrogels is a classical technique for inorganic compounds and biomolecules such as proteins.[11–15] The gel environment can influence the properties[16–22] such as crystal habit, crystal size and polymorphism. Polymorphism depends on a number of factors including the nucleation rate, which can give rise to the simultaneous crystallisation of two or more polymorphs with similar nucleation rates, known as concomitant polymorphism.[23] For decades, researchers have been using various techniques such as evaporative crystallization, solution cooling, melt crystallization and sublimation[24,25] to search for polymorphic modifications. While these methods are highly effective, they can sometimes fail to efficiently isolate slow-nucleating forms. LMWGs can provide various advantages as crystal growth media because of their versatility, stimuli-responsive properties and often facile synthesis. Gel phase crystallisation results in the shutdown of convection currents leading to diffusion limited growth, and the gel fibres can provide an active surface for heterogeneous nucleation. There have been a few recent reports of crystallisation within gels based on LMWGs[21,26–30] and small-molecule supramolecular hydrogels have been used to crystallise pharmaceuticals such a modafinil[26] and carbamazepine.[21] An inert gel matrix based on LMWGs (without drug-specific functionality) has been shown to influence the pharmaceutical crystallisation solid form and habit outcomes.[29] Efforts have also been made to develop supramolecular gel phase crystallisation using a gelator that mimics the anticancer drug cisplatin. This resulted in the crystal habit modification of cisplatin and the isolation of a novel solvate form.[28] LMWGs that are structurally similar to the crystallisation substrate have been shown to give rise to the selective crystallisation of the metastable R polymorph of the highly polymorphic drug precursor ROY.[31] The gel phase crystallisation of isoniazid gives rise to significant differences in the crystal habit and crystal size compared to solution control experiments.[22] In 2004, Hamilton's group demonstrated the use of a hydrogel medium to crystallize calcite,[32] while Gunnlaugsson's group reported that supramolecular gels can be used to produce single crystal nanowires based on NaCl, KCl, and KI in a gel medium.[33] In the present work, we report the use of LMWGs as crystallisation media for coordination compounds, which display several crystalline forms varying in the copper coordination environment. Specifically, we have selected the complexes of copper(II) with isonicotinic acid–*N*-oxide, which exhibits three

[a] *Department of Chemistry, Science Institute, University of Iceland, Dunhagi 3, 107 Reykjavík, Iceland. E-mail: krishna@hi.is; Fax: +354 552 8911; Tel: +354 525 4846*

[b] *Department of Chemistry, Durham University, South Road, Durham DH1 3LE, UK. E-mail: jon.steed@durham.ac.uk*

† Electronic supplementary information (ESI) available: Crystallisation of Cu(II) complexes, details of gelation experiments and gel phase crystallisation, and comparison of PXRD of form-IV. CCDC 1846767. For ESI and crystallographic data in CIF or other electronic format see DOI: 10.1039/c8nj05036h

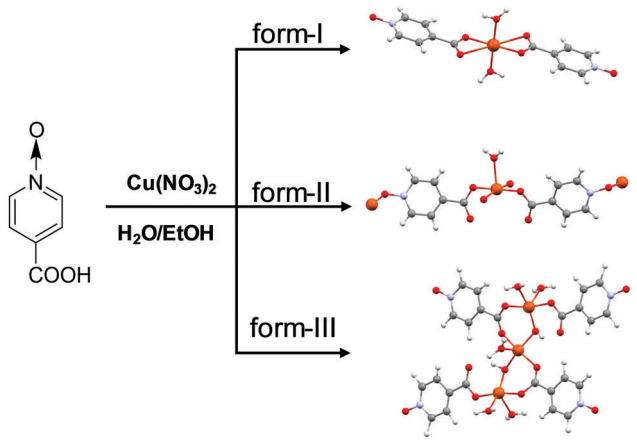

Scheme 1 Molecular structures of three copper(II) isonicotinate–*N*-oxide complexes deposited in the Cambridge Structural Database.[10]

forms[34–36] deposited within the Cambridge Structural Database[10] and these complexes can be easily isolated (Scheme 1). These three forms of the copper(II) isonicotinate–*N*-oxide complex are a discrete square planar diaqua species bound through monodentate carboxylate oxygen atoms $[Cu(C_6H_4NO_3)_2(H_2O)_2]$ (blue, form-I, CSD refcode BUXDED), a square pyramidal aqua complex involving bridging ligands bound by both carboxylate and *N*-oxide oxygen atoms $[Cu(\mu\text{-}C_6H_4NO_3)_2(H_2O)]_n$ (green, form-II, CSD refcode BEJCID) and a trinuclear hydroxyl-bridged species $[Cu(H_2O)(\mu\text{-}OH)_2\{Cu(C_6H_4NO_3)_2(H_2O)_2\}_2]\cdot 2H_2O$ (green, form-III, CSD refcode BULWIO), formed under basic conditions. A fourth form of formula $[\{Cu(C_6H_4NO_3)_2\}\{Cu(C_6H_4NO_3)NO_3\}_2]_n$ (green, form-IV) is reported herein.‡ The gelators are based on the amide N–H···O supramolecular synthon, an important class of stimuli-responsive supramolecular gels[7,37–53] with tuneable properties. Supramolecular gels based on trimesic amide derivatives[33,54–65] have been selected as gel media due to their typically very low minimum gel concentration (MGC). The candidate gel mimicking the pyridine *N*-oxide functional group of the isonicotinic acid–*N*-oxide ligand is reported.

Experimental

Materials and methods

All starting materials were purchased from Sigma Aldrich and were used as supplied. The tris-amide of trimesic acid with L-valine methyl ester (**Val-TMA**)[62] and aminopyridine[54] were synthesised following the reported procedures. The tailored *N*-oxide compound was synthesised by oxidizing the pyridyl group of tris-pyridyl trimesic amide.[54] Deionized water was used for all the experiments and absolute ethanol was obtained by distillation over Mg turnings and iodine.[66] ^{1}H-NMR and ^{13}C-NMR spectra were recorded on a Bruker Advance 400 spectrometer. Single crystal X-ray diffraction (SCXRD) was performed on a Bruker D8 venture, and powder X-ray diffraction (PXRD) was carried out using a Bruker D8 Focus instrument. The morphology of the xerogel was analysed by Scanning Electron Microscopy (SEM) using a Leo Supra 25 Microscope.

Synthesis

3,3′,3″-((Benzene-1,3,5-tricarbonyl)tris(azanediyl))tris-(pyridine 1-oxide) (L-3Nox). To a solution of N^1,N^3,N^5-tri(pyridin-3-yl)benzene-1,3,5-tricarboxamide (0.88 g, 2.0 mmol) in hot methanol (50 mL), *m*-chloroperbenzoic acid (1.86 g, 10.8 mmol) was added in portions over a period of 15 minutes. The reaction mixture was refluxed at 70 °C overnight. The mixture was cooled to room temperature. The solid obtained was filtered, washed with water followed by methanol, dried and the product was obtained as a white powder (0.76 g, 1.6 mmol). Yield: 78.0%. ^{1}H NMR (400 MHz, DMSO-d_6) δ: 10.95 (3H, s), 8.86 (3H, s), 8.74 (3H, s), 8.05 (3H, d, J = 6.4), 7.71 (3H, d, J = 8.4), 7.46 (3H, dd, J = 8.6, 6.2). ^{13}C NMR (100 MHz, DMSO-d_6) δ: 164.78, 138.10, 134.69, 134.40, 131.01, 130.51, 126.23, 116.84. HRMS (m/z) calcd for $C_{24}H_{18}N_6O_6Na$: 509.118; found: 509.118 [M − Na$^+$]. Anal. data for $C_{24}H_{18}N_6O_6$: calc. C, 59.26; H, 3.73; N, 17.28. Found: C, 59.10; H, 3.82; N, 17.00.

$[Cu(C_6H_4NO_3)_2(H_2O)_2]$ (form-I). 27.8 mg (0.2 mmol) of isonicotinic acid–*N*-oxide was dissolved in water (8.5 mL)/ethanol (1.5 mL) mixture and was layered over 5 mL aqueous solution of $Cu(NO_3)_2\cdot 3H_2O$ (24.1 mg, 0.1 mmol). Slow evaporation of the mixture resulted in blue crystals of form-I in 3–4 days.[34]

$[Cu(\mu\text{-}C_6H_4NO_3)_2(H_2O)]_n$ (form-II). 27.8 mg (0.2 mmol) of isonicotinic acid–*N*-oxide was dissolved in ethanol (10 mL) and layered over ethanolic solution (5 mL) of $Cu(NO_3)_2\cdot 3H_2O$ (24.1 mg, 0.1 mmol) and the vial was sealed. Plate shaped green crystals of form-II were obtained in 3–4 days.[36]

$[\{Cu(C_6H_4NO_3)_2\}\{Cu(C_6H_4NO_3)NO_3\}_2]_n$ (form-IV). 27.8 mg (0.2 mmol) of isonicotinic acid–*N*-oxide and 24.1 mg (0.1 mmol) of $Cu(NO_3)_2\cdot 3H_2O$ were added to 2 mL of ethanol and the mixture was heated at 85 °C in a sealed vial. Block shaped green crystals of form-IV were obtained overnight at 85 °C. Anal. data for $C_{24}H_{16}Cu_3N_6O_{18}$: calc. C, 33.25; H, 1.86; N, 9.69. Found: C, 33.16; H, 1.94; N, 9.70.

Single crystal X-ray diffraction

X-ray quality single crystals of form-IV were isolated from mother liquor, immediately immersed in cryogenic oil and then mounted. The diffractions were collected using MoKα radiation (λ = 0.71073 Å) on a Bruker D8 Venture (Photon100 CMOS detector) diffractometer equipped with a Cryostream (Oxford Cryosystems) open-flow nitrogen cryostats at a temperature of 150.0(2) K. The unit cell determination, data collection, data reduction, structure solution/refinement and empirical absorption correction (SADABS) were carried out using Apex-III (Bruker AXS: Madison, WI, 2015). The structure was solved by a direct method and refined by the full-matrix least squares on F^2 for all data using SHELXTL[67] and Olex2[68] software. All non-disordered non-hydrogen

‡ Crystal data for the Cu(II)–isonicotinic acid–*N*-oxide complex (form-IV): $C_{24}H_{16}Cu_3N_6O_{18}$, FW = 867.05, monoclinic, $P2_1/n$, a = 8.892(2), b = 15.096(4), c = 11.178(3) Å, β = 103.646(9)°, V = 3443(3) Å^3, Z = 4, D_c = 1.975 cm^3, F(000) = 866, and T = 150 K. Final residuals (for 242 parameters) were R_1 = 0.0218 for 3288 reflections with $I > 2\sigma(I)$, and R_1 = 0.0218, wR_2 = 0.0581, and GOF = 0.989 for all 3052 reflections. CCDC 1846767 contains the supplementary crystallographic data for this paper.

atoms were refined anisotropically except for the disordered oxygen atom of the nitrate group, where the free variables were refined by the FVAR instruction. All the hydrogen atoms were placed in the calculated positions and refined using a riding model.

Gelation properties of tailored *N*-oxide compounds

The gelating ability of **L-3Nox** was screened in various solvent systems (see the ESI†). The gelator was soluble only in highly polar solvents such as DMF, DMA and DMSO and gels were formed only in DMSO/water mixtures. In a typical experiment, the compound was dissolved in a required amount of DMSO by heating and sonicating followed by the addition of water. The mixture was then sonicated to form a suspension, and left undisturbed to form a gel. The gel formation was confirmed by the inversion test.

Minimum gelation concentration. Various amounts (1.0 to 5.0 mg) of **L-3Nox** gelator were taken in standard vials (7 mL) and 0.5 mL of DMSO was added. The solution was heated and sonicated to dissolve the compound followed by the addition of 0.5 mL water, and the resulting mixture was left undisturbed to form the gel. After 24 hours, the gel formation was checked by an inversion test. The lowest concentration at which the gel was formed was recorded as the minimum gel concentration (MGC).

Gel–sol transition temperature. The required amount of **L-3Nox** gelator was taken in a standard 7 mL vial and the gel was prepared in DMSO/water (1 : 1 v/v) as per the above procedure. After 24 hours, a small spherical glass ball weighing 92.0 mg was placed on the gel surface, and the gel was heated gradually in an oil bath. The temperature at which the ball touched the bottom of the vial was recorded as the gel–sol transition temperature (T_{gel}).

Crystallisation experiments

Crystal-to-crystal transformation: transformation of a blue complex (form-I) to a green polymer (form-II). Form-I (3.0 mg) was added to absolute ethanol (10 mL) in a standard vial. The vial was sealed to prevent the evaporation of ethanol and left without disturbance. Green crystals of form-II were obtained over the course of one week and were characterized by SCXRD.

Transformation of a green polymer (form-II) to a blue complex (form-I). Water (1 mL) was added to form-II (3.0 mg). Excess water was avoided since form-II is sparingly soluble in water. The transparent green crystals almost instantly turned into an opaque blue material and the mixture was left undisturbed. X-ray quality blue crystals of form-I were obtained in 2–3 days and were characterized by SCXRD.

Transformation of a green polymer (form-IV) to a blue complex (form-I). Water (1 mL) was added to form-IV (3.0 mg) in a standard vial. X-ray quality blue crystals were obtained in 2–3 days and characterized by SCXRD.

Scanning electron microscopy. The gelator (**L-3Nox**) was dissolved in 0.7 mL of DMSO, the mixture was heated and sonicated, and 0.3 mL of water was added to form the gel. The gel was filtered through a filter paper after 24 hours and the residue was air-dried in a fume hood. The xerogels were gold coated and SEM was performed using a Leo Supra 25 Microscope.

Gel phase crystallisation

Crystallisation of $Cu(NO_3)_2{\cdot}3H_2O$ and isonicotinic acid–*N*-oxide was performed in the presence of hydrogelators (agarose and gelatin) and low molecular weight gelators (LMWGs). In a typical experiment, isonicotinic acid–*N*-oxide (2 equivalent) and the gelator were dissolved together in water (for agarose and gelatin) and then $Cu(NO_3)_2{\cdot}3H_2O$ (1 equivalent) was added. The solution was sonicated and left undisturbed to form the gel and crystallise. For **Val-TMA** and **L-3Nox**, isonicotinic acid–*N*-oxide and the gelator were dissolved in a polar organic solvent (DMF or DMSO) and $Cu(NO_3)_2{\cdot}3H_2O$ and water were added to this mixture in the quantities given below.

Crystallisation in agarose. Isonicotinic acid–*N*-oxide (13.9 mg, 0.1 mmol) and agarose (6.0 mg) were dissolved in water (1 mL) by heating, and $Cu(NO_3)_2{\cdot}3H_2O$ (12.1 mg, 0.05 mmol) was added to the resulting solution. X-ray quality crystals of form-I were obtained in 2 days.

Gel phase crystallisation in Val-TMA. Isonicotinic acid–*N*-oxide (27.8 mg, 0.2 mmol) and **Val-TMA** (40.0 mg, 4.0 wt%) were dissolved in DMF (0.5 mL) by heating and sonicating. Water (0.5 mL) and $Cu(NO_3)_2{\cdot}3H_2O$ (24.1 mg, 0.1 mmol) were added to this solution, and the mixture was left undisturbed to form a blue gel. X-ray quality crystals of form-I were obtained in 2–3 days.

Gel phase crystallisation in L-3Nox. Isonicotinic acid–*N*-oxide (27.8 mg, 0.2 mmol) and **L-3Nox** (8.0 mg) were dissolved in DMSO (0.5 mL) by heating and sonicating. Water (0.5 mL) and $Cu(NO_3)_2{\cdot}3H_2O$ (24.1 mg, 0.1 mmol) were added to this solution and leaving the mixture undisturbed yielded a blueish green gel. X-ray quality single crystals of form-I were obtained in 2 days.

Results and discussion

Solution phase crystallization

Layering an ethanolic solution of $Cu(NO_3)_2{\cdot}3H_2O$ over an aqueous ethanolic solution (5% of water, v/v) of isonicotinic acid–*N*-oxide at a 1 : 2 metal–ligand ratio results in the formation of a mixture of blue and green crystals over a period of three days (Fig. S1, ESI†). These crystals were isolated, and the structure was determined by single crystal X-ray diffraction. This technique shows that the samples match with the reported structures, namely form-I (blue crystals) and form-II (green crystals).[34,36] Formation of the hydroxyl-bridged species form-III is not expected under these conditions due to the absence of a base.[35] Basic conditions were not investigated because of the effect of changing pH on the gelation process in LMWGs.[69]

We have optimized the crystallisation conditions for these two forms and confirmed that crystallisation depends on the ethanol/water ratio. Form-I can be obtained in aqueous ethanol containing $>10\%$ of water (v/v), whereas the green form-II is formed at lower water content ($<3.5\%$ of water, v/v). Both forms are obtained simultaneously from aqueous ethanol containing 7% water (v/v). The monoaqua form-II transforms into the diaqua form-I over three days, presumably due to the absorption

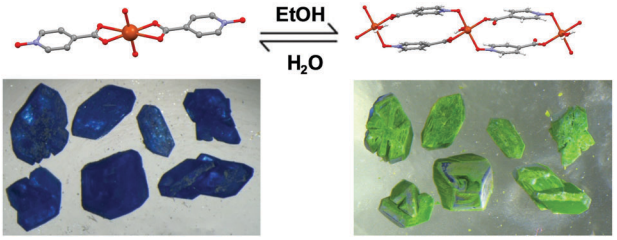

Fig. 1 Solvent mediated crystal-to-crystal transformation of form I and form-II.

of moisture from the mother liquor. The effect of temperature was studied by comparing the room temperature and low temperature (−15 °C) crystallisation for both forms. The yields of the single crystals in both cases were low compared to room temperature crystallisation. We have also performed low temperature crystallisation for form-I and form-II and interestingly, form-II does not disappear from the mixture even after three weeks. The conversion of green to blue crystals prompted us to explore the solvent-mediated solid-state transformation of form-I and form-II. Crystals of form-I were isolated, immersed in absolute ethanol and the crystals underwent conversion to green form-II over five days (Fig. 1). Similarly, treating form-II with water resulted in form-I overnight. The transformation of form-I to form-II was found to be reversible, which was confirmed by single crystal X-ray diffraction.

Heating copper(II) nitrate and isonicotinic acid–*N*-oxide at 85 °C in ethanol in a sealed vial resulted in block-shaped green crystals, a morphology that contrasts to the plate shaped form-II. Single crystal X-ray analysis of the block-shaped green crystals revealed a new coordination polymer (form-IV)‡ of the formula $[\{Cu(C_6H_4NO_3)_2\}\{Cu(C_6H_4NO_3)NO_3\}_2]_n$, which displays two different Cu(II) centres with distorted octahedral and square pyramidal geometries (Fig. 2a). The oxygen atoms of the carboxylate moiety of the isonicotinate–*N*-oxide ligands are coordinated to the two Cu(II) centres in a bidentate fashion forming an eight-membered metallo-macrocycle.

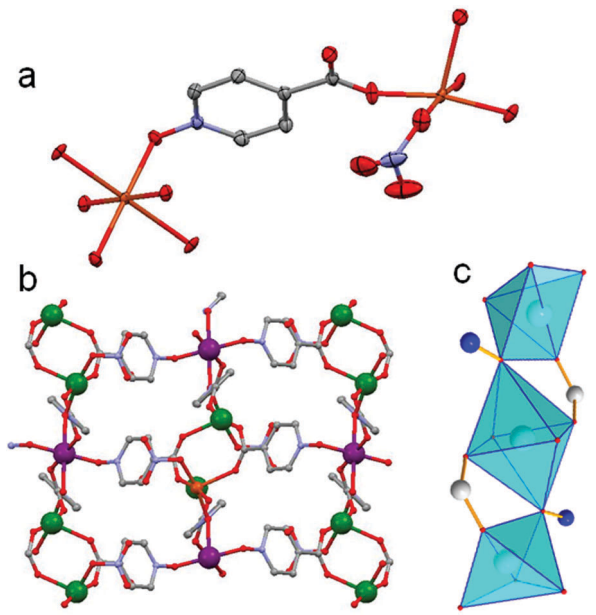

Fig. 2 (a) Molecular structure of form-IV $[\{Cu(C_6H_4NO_3)_2\}\{Cu(C_6H_4NO_3)NO_3\}_2]_n$, (b) representation of crystal structure showing octahedral (purple) and square pyramidal (green) metal centres and (c) interconnected octahedral and square pyramidal geometry.

The Cu(II) centres in the metallo-macrocycle display square pyramidal geometry with oxygen atoms of the *N*-oxide moiety, the nitrate anion and two carboxylate moieties in the equatorial site, and the axial position is coordinated to the oxygen atom of the carboxylate moiety. The oxygen atoms of the *N*-oxide moieties of isonicotinate–*N*-oxide in the metallo-macrocycle are coordinated to the Jahn–Teller distorted octahedral Cu(II) centre. In the octahedral Cu(II) centre, four isonicotinate–*N*-oxide ligands are coordinated to the equatorial position of the metal centre (two oxygen atoms of the *N*-oxide moiety and two carboxylate oxygen atoms), and the axial positions are coordinated to the oxygen atoms of the *N*-oxide moiety. The oxygen atom of the *N*-oxide moiety displays a bridging coordination mode and binds to the equatorial position of the distorted octahedral and square pyramidal copper(II) centres resulting in a complex 3-D network (Fig. 2b). Form-IV was found to convert to form-I when immersed in water (confirmed by single crystal X-ray diffraction).

Gel phase crystallization

The existence of at least four distinct copper(II) isonicotinate–*N*-oxide complexes prompted us to explore the selective crystallisation of this system in gel media. The copper(II) isonicotinate–*N*-oxide compounds were initially crystallised in gels of commercially available hydrogelators, namely agarose and gelatin. A blue gel was obtained by dissolving $Cu(NO_3)_2{\cdot}3H_2O$, isonicotinic acid–*N*-oxide and agarose in hot water, which subsequently produced X-ray quality crystals of blue form-I upon cooling. Crystallisation experiments performed at various concentrations of agarose, $Cu(NO_3)_2{\cdot}3H_2O$ and isonicotinic acid–*N*-oxide gave similar results; however, experiments with low concentration of metal salt and ligand did not yield any solid product. Crystals of isonicotinic acid–*N*-oxide (CSD refcode XUCPAO) were obtained at a higher concentration of metal salt and ligand. Experiments performed with 1 : 1 ethanol/water (v/v) gave similar results. Use of gelatin hydrogels as the crystallization medium resulted in blue gels, but crystals were not formed even after several weeks. Neither gelatin nor agarose formed gels in absolute ethanol. We then turned our attention to LMWGs based on **Val-TMA**[62] (Scheme 2 and ESI†).

Gel phase crystallisation was performed by mixing copper(II) nitrate trihydrate and isonicotinic acid–*N*-oxide at a 1 : 2 metal–ligand ratio with the gelator (4.0 wt%) in ethanol/water and DMF/water (1 : 1, v/v respectively). This resulted in blue crystals of form-I after two days (confirmed by single crystal X-ray diffraction). The formation of form-I in this 'generic' supramolecular gel medium prompted us to investigate the crystallisation of copper(II) isonicotinate–*N*-oxide complexes in the tailored LMWG gel, which is structurally similar to the crystallisation substrate. Recently we have shown that the tailored LMWG gel can enable selective crystallisation[31] of particular

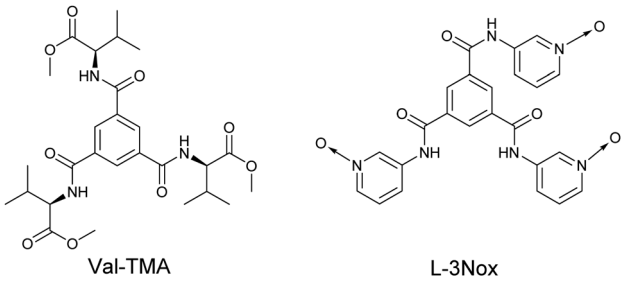

Scheme 2 Chemical structure of a non-tailored gelator (**Val-TMA**) and a tailored *N*-oxide gelator (**L-3Nox**).

polymorphs of the olanzapine precursor, ROY.[70] We have also reported the formation of crystalline materials in a supramolecular gel matrix of copper(II) metallogels with pyridyl amides.[71]

The gelator design involves trimesic pyridyl amide based compounds,[7,37] which show two types of hydrogen bonding motifs, one through a N–H···O synthon involving the amide moiety and the other through a N–H···N synthon involving the amide and the pyridyl ring nitrogen atom. Thus, a tailored gel was designed for the copper(II) isonicotinate–*N*-oxide system by modifying the pyridyl groups of trimesic amides to give *N*-oxides. In this context, we prepared a tailored tris-*N*-oxide compound (**L-3Nox**, Scheme 2) by oxidising *N*,*N*′,*N*″-tris(3-pyridyl)-trimesic amide[54] with *m*-chloroperbenzoic acid (ESI†). The gelation properties of **L-3Nox** were tested in aqueous solutions of highly polar DMSO, due to its poor solubility in other solvents. **L-3Nox** formed gels in various mixtures of DMSO and water (ESI†) and the gel formation was confirmed by an inversion test (Fig. 3). We selected a 7 : 3 DMSO/water mixture (v/v) for **L-3Nox** since the gel was transparent at this composition. The thermal stability of the tailored gel was evaluated by analysing the temperature at which the gel was converted into a liquid phase (T_{gel}). T_{gel} was found to be 107 °C at 0.5 wt% and the minimum gel concentration (MGC) was 0.15 wt% in the DMSO/water (7 : 3, v/v) mixture. T_{gel} and MGC were 105 °C at 0.5 wt% and 0.3 wt% in the 1 : 1 DMSO/water (v/v) mixture. Thus, replacing the pyridyl group with pyridyl *N*-oxide has a significant effect on the MGC of **L-3Nox** (0.15 wt%) compared to *N*,*N*′,*N*″-tris(3-pyridyl)-trimesic amide (0.03 wt%) in the DMSO/water (7 : 3, v/v) mixture.[54]

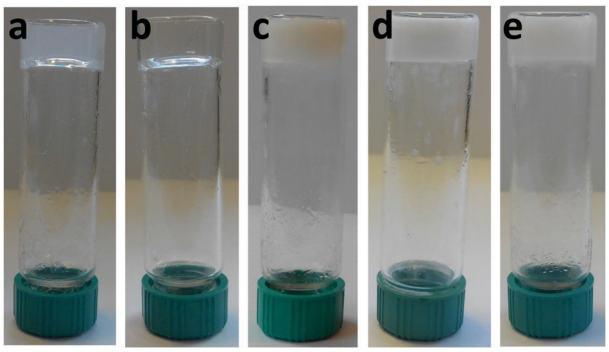

Fig. 3 Gels obtained from (a) agarose in water, (b) gelatin in water, (c) **Val-TMA** in DMF/water (1 : 1 v/v), (d) **Val-TMA** in ethanol and (e) **L-3Nox** in DMSO/water (1 : 1 v/v).

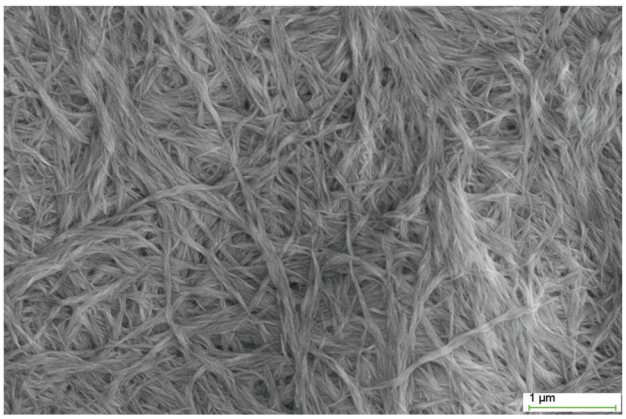

Fig. 4 SEM image of **L-3Nox** xerogel at 0.5 wt% obtained from DMSO/water (7 : 3, v/v).

Scanning electron microscopy (SEM) was performed on the xerogel of **L-3Nox** to elucidate the morphology of the xerogels (Fig. 4), which clearly indicates the fibrous nature of the gel network, and twisted fibres were observed in **L-3Nox**. The thickness of the individual fibres was found to be 20–40 nm and these fibres combine to form bundles with thickness ranging from 100 to 150 nm.

Gel phase crystallisation was performed by mixing copper(II) nitrate trihydrate and isonicotinic acid–*N*-oxide at a 1 : 2 metal–ligand ratio with **L-3Nox** gelator in DMSO/water. The mixture was heated to give a clear green solution and left without disturbing for 2 hours to form the gel (ESI†). The crystallisation experiments were performed at a higher concentration of **L-3Nox** gelator (greater than the MGC) to ensure gel formation. The crystallisation experiments were also performed with varying amounts of copper(II) nitrate trihydrate and isonicotinic acid–*N*-oxide. A greenish-blue gel was formed in an hour in all cases for **L-3Nox** gelator at 0.8 wt% in 1 : 1 (v/v) DMSO/water. The optimized concentration for crystallisation was found to be 0.06 mmol of copper(II) nitrate trihydrate and 0.12 mmol isonicotinic acid–*N*-oxide. Crystals were not formed for experiments with a lower metal–ligand concentration, whereas a concentration of 0.06 mmol or more copper(II) nitrate trihydrate produced blue crystals (form-I) in a week (Fig. 5c).

We have compared the morphologies of form-I crystals obtained from the gel phase crystallisation in different gelators. The solution phase crystallisation in an ethanol/water mixture without a gelator resulted in block shaped crystals. Similar crystals

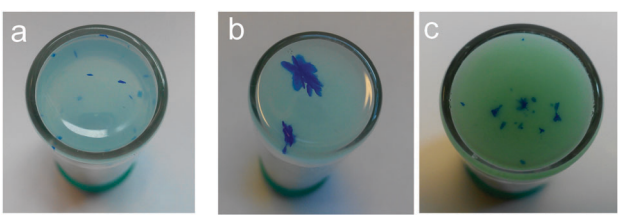

Fig. 5 Gel phase crystallisation of Cu(II) complexes from (a) agarose gel in water (1.5 wt%), (b) **Val-TMA** gel at 4.0 wt% in DMF/water (1 : 1, v/v) and (c) **L-3Nox** gel at 0.8 wt% in DMSO/water (1 : 1, v/v).

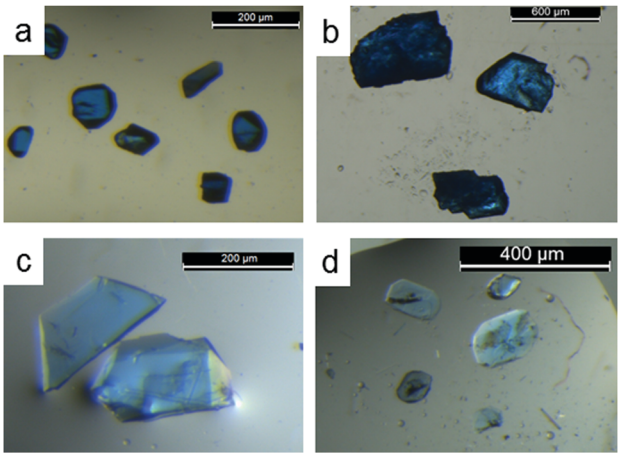

Fig. 6 Images of isolated crystals from (a) solution phase, (b) agarose gel, (c) **Val-TMA** gel and (d) **L-3Nox** gel.

of form-I were obtained in water with very low yield due to the crystallisation of the isonicotinic acid–*N*-oxide ligand. The gel phase crystallisation of the complex in an agarose gel yielded block-shaped crystals (Fig. 6). However, plate shaped crystals were obtained from **Val-TMA** and **L-3Nox** tailored gels indicating that the presence of similar functional groups in the gelator plays a role in crystal morphology. Crystallisation of copper(II) isonicotinate–*N*-oxide complexes was also performed in ethanolic supramolecular gel media. Since the tailored gelator and agarose do not form gels in absolute ethanol or a mixture of ethanol and other solvents, the gel phase crystallisation in ethanol was performed only with **Val-TMA** gelator. Adding copper(II) nitrate to a hot solution of isonicotinic acid–*N*-oxide and **Val-TMA** in absolute ethanol led to a green solution, which subsequently formed a green gel. However, crystals of Cu(II) isonicotinate–*N*-oxide complex were not formed and isonicotinic acid–*N*-oxide crystallised due to its poor solubility in ethanol at ambient temperature. The solubility of isonicotinic acid–*N*-oxide was increased by adding a trace amount of water. Thus, a mixture of isonicotinic acid–*N*-oxide (27.8 mg, 0.2 mmol) and **Val-TMA** (4.0 wt%) was heated in the ethanol/water (5% water, v/v) mixture, and copper(II) nitrate (24.1 mg, 0.1 mmol) was added to yield a green solution and the vial was sealed. The solution turned into a greenish blue gel in 15 minutes, and the blue colour intensified overnight resulting in blue crystals of form-I in the gel medium (Fig. 7a and b). Blue crystals of form-I were formed in almost every case, with one out of 25 trails forming green crystals of form-II, which might be due to accidental heteroseeding. Experiments were performed under identical conditions (the same solvent composition and the same concentration of copper(II) nitrate and isonicotinic acid–*N*-oxide) without **Val-TMA** by adding copper(II) nitrate to a hot solution of isonicotinic acid–*N*-oxide in ethanol/water (5% water, v/v), which resulted in a green solution. The vial was sealed, and a mixture of blue and green crystals was formed overnight (Fig. 7c and d). X-ray single crystal diffraction of these crystals revealed that the blue crystal belongs to form-I and the green crystals were either form-II or form-IV. Thus, concomitant crystallisation of different forms was observed from the solution. Most of the green crystals eventually turned blue over a week.

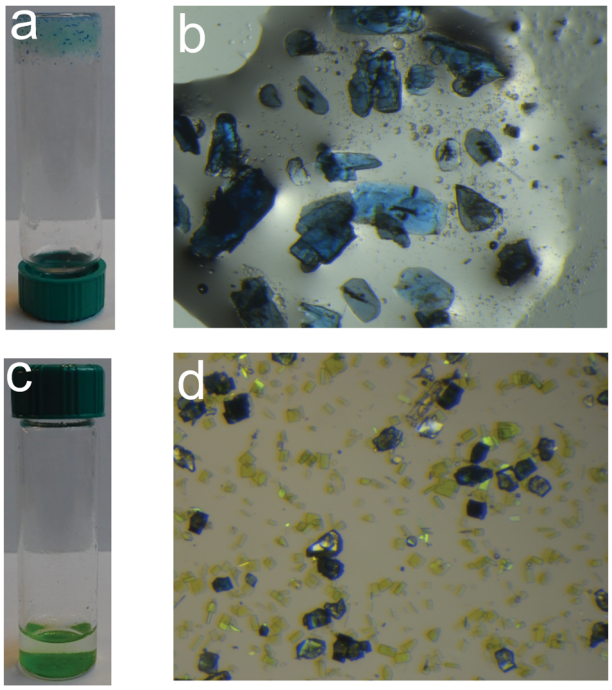

Fig. 7 Crystallisation experiments of the copper(II) isonicotinate–*N*-oxide complex in aqueous ethanol (5% water, v/v) (a) with **Val-TMA** gelator (4.0 wt%) and (b) the isolated crystals. Solution phase crystallisation (c) without gelator and (d) top view of crystals.

Conclusions

In summary, we report the crystallisation of three forms of copper(II) isonicotinate–*N*-oxide (form-I, form-II and form-IV) and their solvent-mediated interconversion. The crystal-to-crystal transformation of a concomitant mixture of blue and green crystals was also studied as a function of solvent concentration. We have designed a gelator that is structurally similar to the crystallisation substrate. Gel phase crystallisation of the complex was performed in hydrogels, the gels of low molecular weight gelators and tailored LMWG. The morphologies of the crystals obtained from solution and from agarose gel proved to be similar to each other while gel phase crystallisation performed in LMWGs and the tailored gelator resulted in plate shaped crystals indicating an influence of the gelator on the crystallization process. Crystallisation of copper(II) isonicotinate–*N*-oxide complexes in aqueous ethanol (5% water, v/v) resulted in a mixture of blue and green crystals, whereas gel phase crystallisation in **Val-TMA** gel under identical conditions resulted in only blue crystals indicating the influence of LMWGs in selective crystallisation of the thermodynamically stable form-I.

Conflicts of interest

There are no conflicts to declare.

Acknowledgements

We thank the University of Iceland Research Fund and the Science Institute for funding and Dr Sigurður Sveinn Jónsson,

ÍSOR-Iceland for powder X-ray diffraction analysis. DG thanks the University of Iceland for the Doctoral Research grant. KF and ZD thank the University of Ljubljana and Vilnius University respectively for the Erasmus exchange program. We thankfully acknowledge Dr Dmitry S. Yufit, the Department of Chemistry, Durham University, UK, for analysing the structures of form-I and form-II and Dr Sigríður Jónsdóttir, University of Iceland, for NMR and mass spectroscopy.

Notes and references

1 L. A. Estroff and A. D. Hamilton, *Chem. Rev.*, 2004, **104**, 1201–1218.
2 M. de Loos, B. L. Feringa and J. H. van Esch, *Eur. J. Org. Chem.*, 2005, 3615–3631.
3 M. George and R. G. Weiss, *Acc. Chem. Res.*, 2006, **39**, 489–497.
4 P. Dastidar, *Chem. Soc. Rev.*, 2008, **37**, 2699–2715.
5 A. R. Hirst, B. Escuder, J. F. Miravet and D. K. Smith, *Angew. Chem., Int. Ed.*, 2008, **47**, 8002–8018.
6 S. Banerjee, R. K. Das and U. Maitra, *J. Mater. Chem.*, 2009, **19**, 6649–6687.
7 M.-O. M. Piepenbrock, G. O. Lloyd, N. Clarke and J. W. Steed, *Chem. Rev.*, 2010, **110**, 1960–2004.
8 D. K. Kumar and J. W. Steed, *Chem. Soc. Rev.*, 2014, **43**, 2080–2088.
9 G. Yu, X. Yan, C. Han and F. Huang, *Chem. Soc. Rev.*, 2013, **42**, 6697–6722.
10 C. R. Groom, I. J. Bruno, M. P. Lightfoot and S. C. Ward, *Acta Crystallogr., Sect. B: Struct. Sci., Cryst. Eng. Mater.*, 2016, **72**, 171–179.
11 H. N. Holmes, *J. Phys. Chem.*, 1916, **21**, 709–733.
12 J. Eckstein, *Cryst. Res. Technol.*, 1996, **31**, 874.
13 M. C. Robert, O. Vidal, J. M. Garcia-Ruiz and F. Otalora, in *Crystallization of Nucleic Acids and Proteins*, ed. M. Ducruix and R. Giegé, Oxford University Press, 2nd edn, 1999, pp. 149–175.
14 M. Conejero-Muriel, J. A. Gavira, E. Pineda-Molina, A. Belsom, M. Bradley, M. Moral, J. d. D. G.-L. Durán, A. Luque González, J. J. Díaz-Mochón, R. Contreras-Montoya, Á. Martínez-Peragón, J. M. Cuerva and L. Álvarez de Cienfuegos, *Chem. Commun.*, 2015, **51**, 3862–3865.
15 T. K. Adalder, D. P. Kumar and P. Dastidar, *Cryst. Growth Des.*, 2014, **14**, 11–14.
16 Z. Yang, H. Gu, Y. Zhang, L. Wang and B. Xu, *Chem. Commun.*, 2004, 208–209.
17 *Polymorphism: In the Pharmaceutical Industry*, Wiley-VCH Verlag GmbH & Co. KGaA, 2006.
18 J. Bernstein, *Polymorphism in Molecular Crystals*, Oxford University Press, 2002.
19 C. Sudha, P. Parimaladevi and K. Srinivasan, *Mater. Sci. Eng., C*, 2015, **47**, 150–155.
20 J. Buendia, E. Matesanz, D. K. Smith and L. Sanchez, *CrystEngComm*, 2015, **17**, 8146–8152.
21 Y. Diao, K. E. Whaley, M. E. Helgeson, M. A. Woldeyes, P. S. Doyle, A. S. Myerson, T. A. Hatton and B. L. Trout, *J. Am. Chem. Soc.*, 2012, **134**, 673–684.
22 S. R. Kennedy, C. D. Jones, D. S. Yufit, C. E. Nicholson, S. J. Cooper and J. W. Steed, *CrystEngComm*, 2018, **20**, 1390–1398.
23 J. Bernstein, R. J. Davey and J.-O. Henck, *Angew. Chem., Int. Ed.*, 1999, **38**, 3440–3461.
24 M. R. Caira, in *Design of Organic Solids*, ed. E. Weber, Y. Aoyama, M. R. Caira, G. R. Desiraju, J. P. Glusker, A. D. Hamilton, R. E. Meléndez and A. Nangia, Springer, Berlin Heidelberg, 1998, pp. 163–208.
25 G. Dhanaraj, K. Byrappa, V. Prasad and M. Dudley, in *Springer Handbook of Crystal Growth*, ed. G. Dhanaraj, K. Byrappa, V. Prasad and M. Dudley, Springer, Berlin Heidelberg, 2010, pp. 3–16.
26 M. Pauchet, T. Morelli, S. Coste, J.-J. Malandain and G. Coquerel, *Cryst. Growth Des.*, 2006, **6**, 1881–1889.
27 F. Aparicio, E. Matesanz and L. Sanchez, *Chem. Commun.*, 2012, **48**, 5757–5759.
28 A. Dawn, K. S. Andrew, D. S. Yufit, Y. Hong, J. P. Reddy, C. D. Jones, J. A. Aguilar and J. W. Steed, *Cryst. Growth Des.*, 2015, **15**, 4591–4599.
29 J. A. Foster, M.-O. M. Piepenbrock, G. O. Lloyd, N. Clarke, J. A. K. Howard and J. W. Steed, *Nat. Chem.*, 2010, **2**, 1037–1043.
30 H. Wang, W. Zhu, J. Li, T. Tian, Y. Lan, N. Gao, C. Wang, M. Zhang, C. F. J. Faul and G. Li, *Chem. Sci.*, 2015, **6**, 1910–1916.
31 J. A. Foster, K. K. Damodaran, A. Maurin, G. M. Day, H. P. G. Thompson, G. J. Cameron, J. C. Bernal and J. W. Steed, *Chem. Sci.*, 2017, **8**, 78–84.
32 L. A. Estroff, L. Addadi, S. Weiner and A. D. Hamilton, *Org. Biomol. Chem.*, 2004, **2**, 137–141.
33 R. Daly, O. Kotova, M. Boese, T. Gunnlaugsson and J. J. Boland, *ACS Nano*, 2013, **7**, 4838–4845.
34 H. Knuuttila and P. Knuuttila, *Acta Chem. Scand., Ser. A*, 1983, **37**, 227–233.
35 H. Knuuttila, *Inorg. Chim. Acta*, 1983, **72**, 11–16.
36 X.-L. Li, J.-T. Chen, D.-Z. Niu, J.-T. Sheng and D.-P. Zhang, *Jiegou Huaxue*, 2003, **22**, 415–418.
37 D. K. Kumar, D. A. Jose, P. Dastidar and A. Das, *Langmuir*, 2004, **20**, 10413–10418.
38 A. Pal, Y. K. Ghosh and S. Bhattacharya, *Tetrahedron*, 2007, **63**, 7334–7348.
39 K. Kawamoto, S. C. Grindy, J. Liu, N. Holten-Andersen and J. A. Johnson, *ACS Macro Lett.*, 2015, **4**, 458–461.
40 Q. Jin, L. Zhang and M. Liu, *Chem. – Eur. J.*, 2013, **19**, 9234–9241.
41 S. Karak, S. Kumar, S. Bera, D. D. Diaz, S. Banerjee, K. Vanka and R. Banerjee, *Chem. Commun.*, 2017, **53**, 3705–3708.
42 K. K. Kartha, V. K. Praveen, S. S. Babu, S. Cherumukkil and A. Ajayaghosh, *Chem. – Asian J.*, 2015, **10**, 2250–2256.
43 Q. Liu, Y. Wang, W. Li and L. Wu, *Langmuir*, 2007, **23**, 8217–8223.
44 K. Ghosh, S. Panja and S. Bhattacharya, *RSC Adv.*, 2015, **5**, 72772–72779.
45 O. Kotova, R. Daly, C. M. G. dos-Santos, M. Boese, P. E. Kruger, J. J. Boland and T. Gunnlaugsson, *Angew. Chem., Int. Ed.*, 2012, **51**, 7208–7212.
46 F. Fages, F. Voegtle and M. Zinic, *Top. Curr. Chem.*, 2005, **256**, 77–131.
47 O. Kotova, R. Daly, C. M. G. dos Santos, P. E. Kruger, J. J. Boland and T. Gunnlaugsson, *Inorg. Chem.*, 2015, **54**, 7735–7741.

48 S. Mukhopadhyay, Ira, G. Krishnamoorthy and U. Maitra, *J. Phys. Chem. B*, 2003, **107**, 2189–2192.
49 K.-P. Tseng, M.-T. Kao, T. W. T. Tsai, C.-H. Hsu, J. C. C. Chan, J.-J. Shyue, S.-S. Sun and K.-T. Wong, *Chem. Commun.*, 2012, **48**, 3515–3517.
50 S. Bhattacharya and S. K. Samanta, *Langmuir*, 2009, **25**, 8378–8381.
51 M. Shirakawa, N. Fujita and S. Shinkai, *J. Am. Chem. Soc.*, 2003, **125**, 9902–9903.
52 U. K. Das, S. Banerjee and P. Dastidar, *Chem. – Asian J.*, 2014, **9**, 2475–2482.
53 H. H. Lee, S. H. Jung, S. Park, K.-M. Park and J. H. Jung, *New J. Chem.*, 2013, **37**, 2330–2335.
54 D. K. Kumar, D. A. Jose, P. Dastidar and A. Das, *Chem. Mater.*, 2004, **16**, 2332–2335.
55 S. Banerjee, N. N. Adarsh and P. Dastidar, *Soft Matter*, 2012, **8**, 7623–7629.
56 N. Shi, G. Yin, H. Li, M. Han and Z. Xu, *New J. Chem.*, 2008, **32**, 2011–2015.
57 T. R. Canrinus, F. J. R. Cerpentier, B. L. Feringa and W. R. Browne, *Chem. Commun.*, 2017, **53**, 1719–1722.
58 R. C. T. Howe, A. P. Smalley, A. P. M. Guttenplan, M. W. R. Doggett, M. D. Eddleston, J. C. Tan and G. O. Lloyd, *Chem. Commun.*, 2013, **49**, 4268–4270.
59 S. Y. Ryu, S. Kim, J. Seo, Y.-W. Kim, O.-H. Kwon, D.-J. Jang and S. Y. Park, *Chem. Commun.*, 2004, 70–71.
60 A. Desmarchelier, M. Raynal, P. Brocorens, N. Vanthuyne and L. Bouteiller, *Chem. Commun.*, 2015, **51**, 7397–7400.
61 F. Camerel and C. F. J. Faul, *Chem. Commun.*, 2003, 1958–1959.
62 Y. Ishioka, N. Minakuchi, M. Mizuhata and T. Maruyama, *Soft Matter*, 2014, **10**, 965–971.
63 J.-L. Zhong, X.-J. Jia, H.-J. Liu, X.-Z. Luo, S.-G. Hong, N. Zhang and J.-B. Huang, *Soft Matter*, 2016, **12**, 191–199.
64 J. J. van Gorp, J. A. J. M. Vekemans and E. W. Meijer, *J. Am. Chem. Soc.*, 2002, **124**, 14759–14769.
65 D. Spitzer, V. Marichez, G. J. M. Formon, P. Besenius and T. M. Hermans, *Angew. Chem., Int. Ed.*, 2018, **57**, 11349–11353.
66 W. L. F. Armarego and C. Chai, *Purification of Laboratory Chemicals*, Butterworth-Heinemann, 5th edn, 2003.
67 G. Sheldrick, *Acta Crystallogr., Sect. C: Cryst. Struct. Commun.*, 2015, **71**, 3–8.
68 O. V. Dolomanov, L. J. Bourhis, R. J. Gildea, J. A. K. Howard and H. Puschmann, *J. Appl. Crystallogr.*, 2009, **42**, 339–341.
69 X. Du, J. Zhou, J. Shi and B. Xu, *Chem. Rev.*, 2015, **115**, 13165–13307.
70 L. Yu, *Acc. Chem. Res.*, 2010, **43**, 1257–1266.
71 D. Ghosh, I. Lebedyte, D. S. Yufit, K. K. Damodaran and J. W. Steed, *CrystEngComm*, 2015, **17**, 8130–8138.

